

1 **CpG-adjuvanted stable prefusion SARS-CoV-2 spike protein protected hamsters**
2 **from SARS-CoV-2 challenge**

3

4 Chia-En Lien¹, Yi-Jiun Lin¹, Charles Chen^{1,2}, Wei-Cheng Lian¹, Tsun-Yung Kuo^{1,3}, John D
5 Campbell⁴, Paula Traquina⁴, Meei-Yun Lin¹, Luke Tzu-Chi Liu¹, Ya-Shan Chuang¹, Hui-Ying Ko⁵,
6 Chun-Che Liao⁵, Yen-Hui Chen⁵, Jia-Tsong Jan⁶, Cheng-Pu Sun⁵, Yin-Shiou Lin⁵, Ping-Yi Wu⁵,
7 Yu-Chiuang Wang⁵, Mi-Hua Tao^{5,7*}, Yi-Ling Lin^{5,7*}

8

9 ¹Medigen Vaccine Biologics Corporation, Taipei City, Taiwan

10 ²Temple University, Philadelphia, PA 19122, USA

11 ³Department of Biotechnology and Animal Science, National Ilan University, Yilan County, Taiwan

12 ⁴Dynavax Technologies, Emeryville, CA 94608, USA

13 ⁵Institute of Biomedical Sciences, Academia Sinica, Taipei, Taiwan

14 ⁶Genomic Research Center, Academia Sinica, Taipei, Taiwan

15 ⁷Biomedical Translation Research Center, Academia Sinica, Taipei, Taiwan

16 *Corresponding authors: bmtao@ibms.sinica.edu.tw, yll@ibms.sinica.edu.tw

17

18

19

20

21

22

23

24

25

26

27

28

29

30

31

32

33

34 **Abstract**

35 The COVID-19 pandemic presents an unprecedented challenge to global public health. Rapid
36 development and deployment of safe and effective vaccines are imperative to control the pandemic. In the
37 current study, we applied our adjuvanted stable prefusion SARS-CoV-2 spike (S-2P)-based vaccine,
38 MVC-COV1901, to hamster models to demonstrate immunogenicity and protection from virus challenge.
39 Golden Syrian hamsters immunized intramuscularly with two injections of 1 µg or 5 µg of S-2P adjuvanted
40 with CpG 1018 and aluminum hydroxide (alum) were challenged intranasally with SARS-CoV-2. Prior to
41 virus challenge, the vaccine induced high levels of neutralizing antibodies with 10,000-fold higher IgG level
42 and an average of 50-fold higher pseudovirus neutralizing titers in either dose groups than vehicle or adjuvant
43 control groups. Six days after infection, vaccinated hamsters did not display any weight loss associated with
44 infection and had significantly reduced lung pathology and most importantly, lung viral load levels were
45 reduced to lower than detection limit compared to unvaccinated animals. Vaccination with either 1 µg or 5 µg
46 of adjuvanted S-2P produced comparable immunogenicity and protection from infection. This study builds
47 upon our previous results to support the clinical development of MVC-COV1901 as a safe, highly
48 immunogenic, and protective COVID-19 vaccine.

49 **Introduction**

50 With over 80 million cases and more than 1.8 million deaths worldwide as of the end of 2020, the
51 COVID-19 pandemic continues to ravage the world one year after its first report in December 2019 [1, 2]. The
52 pandemic also spurred a hitherto unheard of rate of research and vaccine development with 172 vaccines in
53 preclinical development and 61 vaccines in clinical development according to the WHO in December 2020 [3].
54 The rapid progress of COVID-19 vaccine developed is tracked, for example, by the New York Times's
55 COVID-19 Vaccine Tracker, which continuously track and update progress of vaccine development and
56 approval [4]. Clearly, the monumental task of controlling this pandemic on a global scale and immunizing a
57 population over 7 billion will require more than a few types of vaccines.

58 The vast majority of COVID-19 vaccines use the full length or the receptor binding domain of spike (S)
59 protein on the surface of the virus as the antigen, as this binds to human angiotensin converting enzyme 2
60 (hACE2) for cellular entry and is the major neutralizing antibody inducing antigen [5]. Various modifications
61 including modification of two prolines and inactivation of the furin site have been made to the S protein to
62 lock in its prefusion form to enhance its stability and immunogenicity, and this has been applied to current
63 vaccine development [6-9]. We have previously reported preclinical immunogenicity and safety results of
64 prefusion stabilized S protein, S-2P, adjuvanted with CpG 1018 and aluminum hydroxide (alum) in rodent
65 models [10]. The adjuvanted S-2P (MVC-COV1901) was highly immunogenic and promoted a Th1-biased
66 immune response in mice and no serious adverse effects were observed in toxicology studies in rats [10].
67 Based on these results, we have carried out the current study in order to investigate the *in vivo* efficacy of
68 MVC-COV1901 in an animal model which is permissive to SARS-CoV-2 and displays symptoms of
69 infection.

70 Although non-human primates have been used for challenge studies involving SARS-CoV-2 due to
71 similarity of ACE2 receptors and relative closeness to human, the limited availability and high cost are
72 increasingly prohibitive [11]. Small rodent models provide a more economical means of studying the virus;
73 however, mouse ACE2 receptors do not allow permissive infection of SARS-CoV-2 and genetic modification
74 of mice to express human ACE2 (hACE2) or transient transduction using adenovirus-associated virus (AAV)

75 of hACE2 are laborious and costly [12]. Golden Syrian hamsters were found to have the closest homologue of
76 hACE2 and can be infected in lower respiratory tract presenting with symptoms such as weight loss,
77 respiratory distress and lung injury, thus making them an attractive small animal model with which to study
78 SARS-CoV-2 challenge and vaccine development [12-14].

79 In this study, we present data from a hamster challenge study to test MVC-COV1901 using CpG 1018 and
80 alum adjuvanted S-2P. Potent immunogenicity was induced and hamsters were protected from SARS-CoV-2
81 infection as demonstrated by the findings that (a) no decreases in body weight were observed in hamsters
82 immunized with both low and high dosage of the vaccine candidate antigen; (b) virus was undetectable in the
83 lungs of immunized hamsters at 3 days after infection by fifty-percent tissue culture infective dose (TCID₅₀);
84 and (c) immunized hamsters were protected from lung injury at 6 days after challenge, precluding potential
85 vaccine-associated enhanced respiratory disease (VAERD). These results provide additional evidence for the
86 advancement of our clinical development of MVC-COV1901, of which a phase II trial is current underway
87 (NCT04695652).

88

89 **Results**

90 **Hamsters as SARS-CoV-2 virus challenge model for MVC-COV1901**

91 To develop a SARS-CoV-2 virus challenge model in hamsters for MVC-COV1901, an initial study was
92 conducted to determine the optimal dose of virus for the challenge experiments. Unvaccinated hamsters were
93 inoculated with 10³, 10⁴, or 10⁵ PFU of SARS-CoV-2 and euthanized on Day 3 or 6 after infection for tissue
94 sampling (Figure S1). Following infection of 10³ to 10⁵ PFU of SARS-CoV-2, the hamsters exhibited
95 dose-dependent weight loss. Hamsters infected with 10³ PFU gained weight while 10⁴ and 10⁵ PFU-infected
96 hamsters experienced progressively severe weight loss at 6 days post-infection (d.p.i.) (Figure S2). However,
97 there were no significant differences between levels of viral genome RNA (Figure S3a) and viral titer (Figure
98 S3b) measured in 10³ to 10⁵ PFU of SARS-CoV-2-infected hamsters at 3 and 6 d.p.i. All dosages of virus
99 resulted in elevated lung pathology (Figure S4), even at 10³ PFU where the animals did not experience weight
100 loss (Figure S2). There was also no virus inoculation dose-dependent effect on lung pathology scores and lung

101 viral load (Figures S3, S4). Therefore 10^4 PFU of virus was used for virus challenge studies as it provides an
102 adequate balance between clinical signs and virus titer for inoculation.

103

104 **Administration of S-2P adjuvanted with CpG 1018 and aluminum hydroxide to hamsters induced high** 105 **levels of neutralizing antibodies**

106 The main study is outlined as in Figure 1: Hamsters were divided into four groups receiving two
107 immunizations at 21 days apart of either vehicle control (PBS only), adjuvant alone, low dose (LD) or high
108 dose (HD) of MVC-COV1901. No differences in body weight changes were observed after vaccination
109 among the four groups (Figure S5). Fourteen days after the second immunization, high level of neutralizing
110 antibody titers were found in both LD and HD groups with ninety-percent inhibition dilution (ID_{90}) geometric
111 mean titer (GMT) of 2,226 and 1,783, respectively (Figure 2a). Anti-S IgG antibody levels were high enough
112 that several individual samples reached the upper threshold of detection, with GMTs of LD and HD groups of
113 1,492,959 and 1,198,315, respectively (Figure 2b). In general, even at low dose, MVC-COV1901 induced
114 potent levels of immunogenicity in hamsters.

115

116 **Adjuvanted S-2P protected hamsters from clinical signs and viral load after SARS-CoV-2 challenge**

117 Four weeks after the second immunization, hamsters were challenged with 10^4 PFU of SARS-CoV-2
118 virus and body weights were tracked up to 3 or 6 days post infection (d.p.i.). Groups of animals were
119 sacrificed on 3 or 6 d.p.i. for viral load and histopathology analyses (Figure 1). LD and HD vaccinated groups
120 did not show weight loss up to 3 or 6 days after virus challenge and instead gained 5 and 3.8 g of mean weight
121 at 6 d.p.i., respectively (Figure 3). The protective effect was most significant at 6 d.p.i. in both vaccinated
122 groups, while vehicle control and adjuvant only groups experience significant weight loss (Figure 3). Lung
123 viral load measured by viral RNA and $TCID_{50}$ assays showed that both viral RNA and viral titer decreased
124 significantly at 3 d.p.i. in vaccinated hamsters and dropped to below the lower limit of detection at 6 d.p.i.
125 (Figure 4). Note that viral load, especially viral titer measured by $TCID_{50}$ dropped noticeably at 6 d.p.i. in
126 control and adjuvant only groups due to hamsters' natural immune response (Figure 4). Lung sections were

127 analyzed and pathology scoring was tabulated (Figure 5). There were no differences at 3 d.p.i. between
128 control and experimental groups; however, at 6 d.p.i., the vehicle control and adjuvant only groups had
129 significantly increased lung pathology including extensive immune cell infiltration and diffuse alveolar
130 damage, compared to the HD antigen/adjuvant immunized groups (Figure 5, S6). These results showed that
131 MVC-COV1901-induced robust immunity was able to suppress viral load in lungs and prevent weight loss
132 and lung pathology in infected hamsters.

133

134

135 **Discussion**

136 This report contains the first *in vivo* study that evaluates the preclinical efficacy of MVC-COV1901. A
137 preliminary study helped identify the optimal timing for the observation of change of viral load as measured
138 by viral RNA and infectious virus dose (TCID₅₀), which was 3 d.p.i., and 6 d.p.i., respectively. The assays
139 established by Academia Sinica allowed for the observation of a wide window of viral load using both
140 RT-qPCR or TCID₅₀. No infectious virus was detected after 3 d.p.i. in hamsters immunized with low dose or
141 high dose of MVC-COV1901, while the low dose arm showed positive for viral RNA at 3 d.p.i.. The
142 discrepancy could be a result of any remaining inoculated virus or virus inactivated by the antibodies. The
143 measurement of sub-genomic RNA (sgRNA) could have helped distinguish the amplifying virus from
144 inactivated virus [15]. All of the hamsters in the MVC-COV1901-immunized groups were protected with
145 significantly reduced lung pathology (generally graded minimal to mild, with a mean score of 1.72 in LD and
146 HD groups), in contrast to diffuse alveolar damage (graded moderate to severe, with a mean score of 4.09 in
147 vehicle and adjuvant control groups) caused by the virus in the lungs of hamsters, in the control groups at 6
148 d.p.i.. The significance of this study lies not only in the demonstration of *in vivo* efficacy, but also in safety.
149 The viral challenge study allowed for the assessment of risk of disease enhancement with the vaccine
150 candidate. The histopathology scores of the immunized groups have not differed from the non-challenged
151 animals; no evidence of vaccine enhancement was found. Following the consensus made by CEPI and
152 Brighton Collaboration in March 2020, the animal study was run in parallel while Phase I study was

153 cautiously proceeding with careful review of safety data [16]. The vaccines used in this study are from the
154 same batch as the ones used in our Phase I study [17]. The result of this study provides more data that
155 supports progression of the vaccine candidate's clinical development. There are a few limitations of this study.
156 Firstly, the hamsters were challenged with SARS-CoV-2 at 29 days after the second immunization, a
157 relatively short time that did not allow for the evaluation of the durability of protective antibodies. Secondly,
158 none of the animals died in the pre-test or challenge study within the observation time. Thus, the model is not
159 suitable for the evaluation of severe disease or mortality prevention but, rather, is appropriate for evaluation of
160 the effects of immunization on viral challenge-induced moderate disease. Thirdly, nasal swab was not
161 conducted, thus the study did not evaluate the vaccine's ability to block viral entry or prevent upper
162 respiratory tract infection. Further studies are needed to evaluate the durability of the protective antibody, the
163 capacity of MVC-COV1901 to prevent severe disease, mortality, or viral entry.

164

165 **Methods**

166 **Production of S-2P protein ectodomains from ExpiCHO-S cells**

167 SARS-CoV-2 (Wuhan-Hu-1 strain, GenBank: MN908947) S-2P proteins containing residues 1–1208
168 with a C-terminal T4 fibrin trimerization domain, an HRV3C cleavage site, an 8×His-tag and a
169 Twin-Strep-tag were produced in ExpiCHO-S cells (ThermoFisher) as described previously [10].

170

171 **Pseudovirus-based neutralization assay and IgG ELISA**

172 Lentivirus expressing the Wuhan-Hu-1 strain SARS-CoV-2 spike protein was constructed and the
173 neutralization assay performed as previously described [10]. Briefly, HEK293-hACE2 cells were seeded in
174 96-well white isoplates and incubated overnight. Sera from vaccinated and unvaccinated hamsters were
175 heat-inactivated and diluted in MEM supplemented with 2% FBS at an initial dilution factor of 20, and then
176 2-fold serial dilutions were carried out for a total of 8 dilution steps to a final dilution of 1:5120. The diluted
177 sera were mixed with an equal volume of pseudovirus (1,000 TU) and incubated at 37 °C for 1 hour before
178 adding to the plates with cells. Cells were lysed at 72 hours post-infection and relative luciferase units (RLU)

179 was measured. The 50% and 90% inhibition dilution titers (ID₅₀ and ID₉₀) were calculated referencing
180 uninfected cells as 100% neutralization and cells transduced with only virus as 0% neutralization. Total serum
181 anti-S IgG titers were detected with direct ELISA using custom 96-well plates coated with S-2P antigen.

182

183 **Animals and ethical statements**

184 Female golden Syrian hamsters aged 6-9 weeks old on study initiation were obtained from the National
185 Laboratory Animal Center (Taipei, Taiwan). Animal immunizations were conducted in the Testing Facility for
186 Biological Safety, TFBS Bioscience Inc., Taiwan. At 3 weeks after the second immunization, the animals
187 were transferred to Academia Sinica, Taiwan for SARS-CoV-2 challenge. All procedures in this study
188 involving animals were conducted in a manner to avoid or minimize discomfort, distress, or pain to the
189 animals. All animal work in the current study was reviewed and approved by the Institutional Animal Care
190 and Use Committee (IACUC) with animal study protocol approval number TFBS2020-019 and Academia
191 Sinica (approval number: 20-10-1526).

192

193 **Immunization and challenge of hamsters**

194 The hamsters were randomized from different litters into four groups (n=10 for each group): hamsters
195 were vaccinated intramuscularly with 2 injections of vehicle control (PBS), 1 or 5 µg of S-2P protein
196 adjuvanted with 150 µg CpG 1018 and 75 µg aluminum hydroxide (alum), or adjuvant alone at 3 weeks apart.
197 The hamsters were bled at 2 weeks after the second immunization via submandibular vein to confirm presence
198 of neutralizing antibodies. Hamsters were challenged at 4 weeks after the second immunization with 1 x 10⁴
199 PFU of SARS-CoV-2 TCDC#4 (hCoV-19/Taiwan/4/2020, GISAID accession ID: EPI_ISL_411927)
200 intranasally in a volume of 100 µL per hamster. The hamsters were divided into two cohorts to be euthanized
201 on 3 and 6 days after challenge for necropsy and tissue sampling. Body weight and survival rate for each
202 hamster were recorded daily after infection. On days 3 and 6 after challenge, hamsters were euthanized by
203 carbon dioxide. The right lung was collected for viral load determination (RNA titer and TCID₅₀ assay). The
204 left lung was fixed in 4% paraformaldehyde for histopathological examination.

205

206 **Quantification of viral titer in lung tissue by cell culture infectious assay (TCID₅₀)**

207 The middle, inferior, and post-caval lung lobes of hamsters were homogenized in 600 µl of DMEM with
208 2% FBS and 1% penicillin/streptomycin using a homogenizer. Tissue homogenate was centrifuged at 15,000
209 rpm for 5 minutes and the supernatant was collected for live virus titration. Briefly, 10-fold serial dilutions of
210 each sample were added onto Vero E6 cell monolayer in quadruplicate and incubated for 4 days. Cells were
211 then fixed with 10% formaldehyde and stained with 0.5% crystal violet for 20 minutes. The plates were
212 washed with tap water and scored for infection. The fifty-percent tissue culture infectious dose (TCID₅₀)/mL
213 was calculated by the Reed and Muench method [18].

214

215 **Real-time RT-PCR for SARS-CoV-2 RNA quantification**

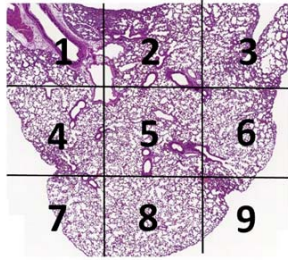
216 To measure the RNA levels of SARS-CoV-2, specific primers targeting 26,141 to 26,253 region of the
217 envelope (E) gene of SARS-CoV-2 genome were used by TaqMan real-time RT-PCR method described in the
218 previous study [19]. Forward primer E-Sarbeco-F1 (5'-ACAGGTACGTTAATAGTTAATAGCGT-3') and
219 the reverse primer E-Sarbeco-R2 (5'-ATATTGCAGCAGTACGCACACA-3'), in addition to the probe
220 E-Sarbeco-P1 (5'-FAM-ACACTAGCCATCCTTACTGCGCTTCG-BBQ-3') were used. A total of 30 µL
221 RNA solution was collected from each lung sample using RNeasy Mini Kit (QIAGEN, Germany) according
222 to the manufacturer's instructions. Five µL of RNA sample was added into a total 25 µL mixture of the
223 Superscript III one-step RT-PCR system with Platinum Taq Polymerase (Thermo Fisher Scientific, USA). The
224 final reaction mix contained 400 nM forward and reverse primers, 200 nM probe, 1.6 mM of
225 deoxy-ribonucleoside triphosphate (dNTP), 4 mM magnesium sulfate, 50 nM ROX reference dye, and 1 µL of
226 enzyme mixture. Cycling conditions were performed using a one-step PCR protocol: 55°C for 10 min for
227 first-strand cDNA synthesis, followed by 3 min at 94°C and 45 amplification cycles at 94°C for 15 sec and
228 58°C for 30 sec. Data was collected and calculated by Applied Biosystems 7500 Real-Time PCR System
229 (Thermo Fisher Scientific, USA). A synthetic 113-bp oligonucleotide fragment was used as a qPCR standard

230 to estimate copy numbers of the viral genome. The oligonucleotides were synthesized by Genomics BioSci
231 and Tech Co. Ltd. (Taipei, Taiwan).

232 **Histopathology**

233 The left lung of hamsters was isolated and fixed in 4% paraformaldehyde. After fixation with 4%
234 paraformaldehyde for one week, the lung was trimmed, processed, embedded, sectioned, and stained with
235 Hematoxylin and Eosin (H&E), followed by microscopic examination. The lung section was evaluated with a
236 lung histopathological scoring system described below [20, 21]:

237 Lung section is divided into 9 areas and numbered as in the example below:



238
239 Lung tissue of every area is scored using the following scoring system in the Table 1.

240 The average of scores of these 9 areas is used to represent the score of the animal.

Score	Observations
0	Normal, no significant finding
1	Minor inflammation with slight thickening of alveolar septa and sparse monocyte infiltration
2	Apparent inflammation, alveolus septa thickening with more interstitial mononuclear inflammatory infiltration
3	DAD*, with alveolus septa thickening, and increased infiltration of inflammatory cells
4	DAD, with extensive exudation and septa thickening, shrinking of alveoli, restricted fusion of the thick septa, obvious septa hemorrhage and more cell infiltration in alveolar cavities
5	DAD, with massive cell filtration in alveolar cavities and alveoli shrinking, sheets of septa fusion, and hyaline membranes lining the alveolar walls

241 *DAD = Diffuse alveolar damage

242 **Table 1.** Lung histopathology scoring system

243

244 **Statistical analysis**

245 The analysis package in Prism 6.01 (GraphPad) was used for statistical analysis. One-way and two-way
246 ANOVA with Tukey's multiple comparison test and Kruskal-Wallis with corrected Dunn's multiple
247 comparisons test were used to calculate significance as noted in respective figure descriptions. * = $p < 0.05$,
248 ** = $p < 0.01$, *** = $p < 0.001$, **** = $p < 0.0001$

249

250 **Acknowledgements**

251 We are grateful for the participation of Dr. Michael D. Malison and Dr. Robert L. Coffman for
252 manuscript review and constructive comments, and Wendy Li for organizing the lung histopathology figures.
253 We also thank team members at TFBS Bioscience Incorporation for hamster housing and immunization
254 process. We thank the Biosafety Level 3 Facility, Academia Sinica, Taiwan, for providing environment to
255 handling and performing wild-type virus assay and Dr. Yu-Chi Chou at the RNAi Core Facility, Academia
256 Sinica for the pseudovirus neutralization assay.

257

258 **Author Contributions**

259 T.-Y. K. produced the S-2P antigens used in the study. C.-E. L., Y.-J. L., J. D. C., P. T., M.-Y. L., M.-H.
260 T., and Y.-L. L. designed the study and experiments. C.-E. L., Y.-J. L., H.-Y. K., C.-C. L., Y.-H. C., J.-T. J.,
261 C.-P. S., Y.-S. L., P.-Y. W., and Y.-C. W. performed and analyzed the experiments. M.-Y. L., L. T.-C. L., and
262 Y.-S. C. drafted the manuscript. All authors reviewed and approved of the final version of the manuscript.

263

264 **Competing Interests**

265 The authors declare no competing interests.

266

267 **Data Availability**

268 The datasets generated during and/or analyzed during the current study are available from the
269 corresponding author on reasonable request.

270

271

272

273 **References**

- 274 1. Dong, E., Du, H. & Gardner, L. An interactive web-based dashboard to track COVID-19 in real time. *Lancet*
275 *Inf Dis.* 20(5), 533-534 (2020).
- 276 2. Gates B. Responding to Covid-19—a once-in-a-century pandemic? *N. Engl. J. Med.* 382(18), 1677-9 (2020).
- 277 3. WHO R&D Blueprint. Landscape of COVID-19 Candidate Vaccines – 22 December 2020. Available from:
278 <https://www.who.int/who-documents-detail/draft-landscape-of-covid-19-candidate-vaccines> (2020)
- 279 4. Zimmer, C., Corum J., & Wee, S. Coronavirus Vaccine Tracker, *The New York Times*.
280 <https://www.nytimes.com/interactive/2020/science/coronavirus-vaccine-tracker.html> (2020)
- 281 5. Krammer, F. SARS-CoV-2 vaccines in development. *Nature* 586, 516–527 (2020).
282 <https://doi.org/10.1038/s41586-020-2798-3>
- 283 6. Wrapp, D. *et al.* Cryo-EM structure of the 2019-nCoV spike in the prefusion conformation. *Science*.
284 367(6483), 1260-3 (2020).
- 285 7. Hsieh, C. L. *et al.* Structure-based design of prefusion-stabilized SARS-CoV-2 spikes. *bioRxiv*.
286 2020.05.30.125484 (2020).
- 287 8. Tian, J. H. *et al.* SARS-CoV-2 spike glycoprotein vaccine candidate NVX-CoV2373 elicits immunogenicity in
288 baboons and protection in mice. *bioRxiv*. 2020.06.29.178509 (2020).
- 289 9. Liang, J. G. *et al.* S-Trimer, a COVID-19 subunit vaccine candidate, induces protective immunity in
290 nonhuman primates. *bioRxiv*. 2020.09.24.311027
- 291 10. Kuo, T.-Y. *et al.* Development of CpG-adjuvanted stable prefusion SARS-CoV-2 spike antigen as a subunit
292 vaccine against COVID-19. *Sci Rep* 10, 20085 (2020). <https://doi.org/10.1038/s41598-020-77077-z>
- 293 11. <https://www.theatlantic.com/science/archive/2020/08/america-facing-monkey-shortage/615799/>
- 294 12. Munoz-Fontela, C. *et al.* Animal models for COVID-19. *Nature* 586, 509–515 (2020).
295 <https://doi.org/10.1038/s41586-020-2787-6>
- 296 13. Imai M. *et al.* Syrian hamsters as a small animal model for SARS-CoV-2 infection and countermeasure
297 development. *Proc Natl Acad Sci.* 117(28):16587 (2020)
- 298 14. Sia, S. F. *et al.* Pathogenesis and transmission of SARS-CoV-2 in golden hamsters. *Nature* 583, 834–838
299 (2020). <https://doi.org/10.1038/s41586-020-2342-5>
- 300 15. Woelfel R. *et al.* Clinical presentation and virological assessment of hospitalized cases of coronavirus disease
301 2019 in a travel-associated transmission cluster. *medRxiv* 2020.03.05.20030502
- 302 16. Lambert P.-H. *et al.* Consensus summary report for CEPI/BC March 12–13, 2020 meeting: Assessment of risk
303 of disease enhancement with COVID-19 vaccines, *Vaccine* 38(31):4783-4791 (2020)
- 304 17. <https://clinicaltrials.gov/ct2/show/NCT04487210?term=medigen&cntry=TW&draw=2&rank=2>
- 305 18. Reed L. J. And Muench H. A simple method of estimating fifty per cent endpoints. *American journal of*
306 *epidemiology.* 1938 May 1;27(3):493-7.

- 307 19. Corman V. M. *et al.* Detection of 2019 novel coronavirus (2019-nCoV) by real-time RT-PCR.
308 Eurosurveillance. 2020 Jan 23;25(3):2000045.
- 309 20. Liu L. *et al.* Anti-spike IgG causes severe acute lung injury by skewing macrophage responses during acute
310 SARS-CoV infection. JCI Insight. 2019 Feb 21;4(4):e123158.
- 311 21. Jiang R.D. *et al.* Pathogenesis of SARS-CoV-2 in transgenic mice expressing human angiotensin-converting
312 enzyme 2. Cell. 2020 Jul 9;182(1):50-8.

313

314

315

316

317

318

319

320

321

322

323

324

325

326

327

328

329

330

331

332

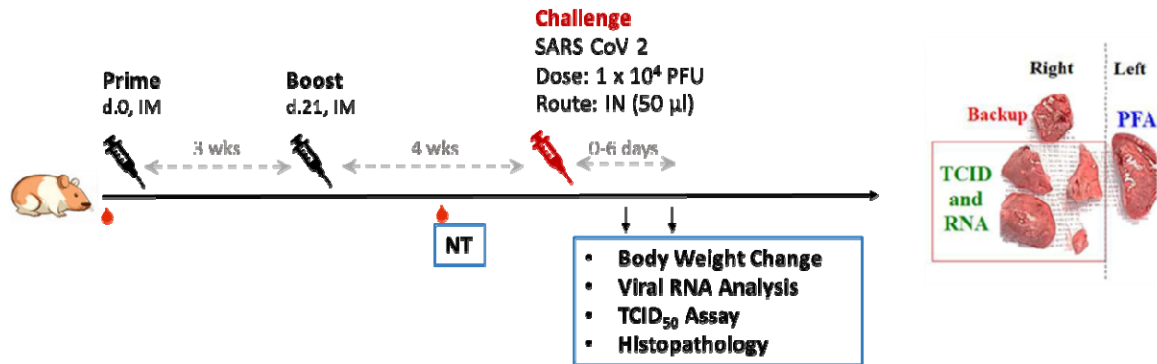
333

334

335

336 **Figures**

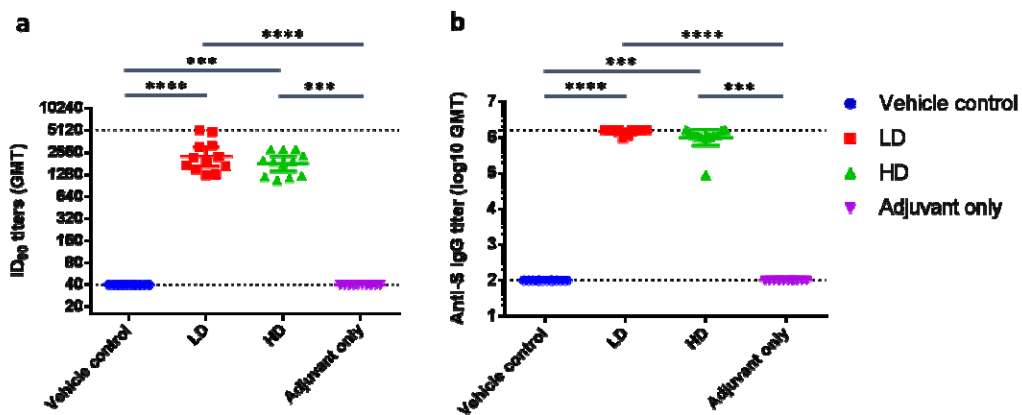
337



338

339 **Figure 1. Study design of the hamster challenge study.**

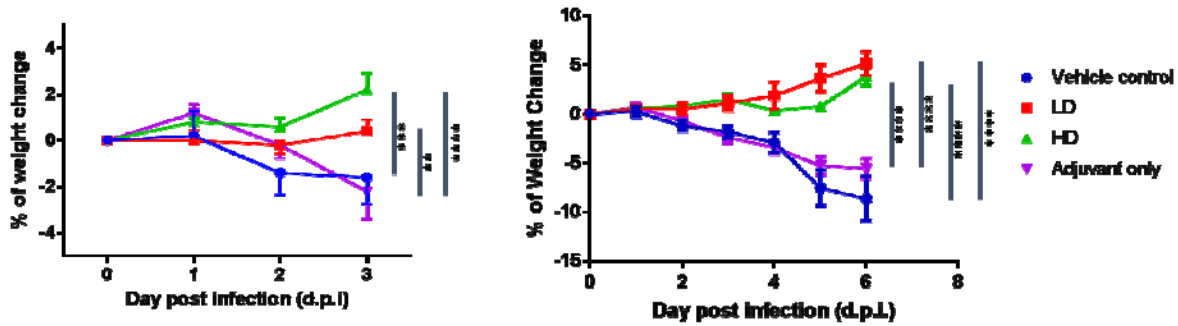
340 Hamsters were immunized twice at 3 weeks apart and 2 weeks after the second immunization, serum
 341 samples were taken for immunogenicity assays. Four weeks after the second immunization, hamsters were
 342 challenged with 10^4 PFU of SARS-CoV-2. Body weights were tracked for 3 to 6 days after infection and the
 343 animals were euthanized on the third or sixth day after infection for necropsy and tissue sampling.



344

345 **Figure 2. Neutralizing antibody titers with pseudovirus assay in hamsters 2 weeks after second**

346 **immunization.** Hamsters (N=10 per group) were immunized twice at 3 weeks apart with vehicle control
 347 (PBS), 1 µg (LD) or 5 µg (HD) of S-2P adjuvanted with 150 µg CpG 1018 and 75 µg aluminum hydroxide, or
 348 with adjuvant alone. The antisera were harvested at 2 weeks after the second injection and subjected to **a.**
 349 neutralization assay with pseudovirus expressing SARS-CoV-2 spike protein to determine the ID₉₀ titers of
 350 neutralization antibodies and **b.** total anti-S IgG antibody titers with ELISA. Results are presented as
 351 geometric mean with error bars representing 95% confidence interval and statistical significance calculated
 352 with Kruskal-Wallis with corrected Dunn's multiple comparisons test. Dotted lines represent lower and upper
 353 limits of detection (40 and 5120 in ID₉₀, 100 and 1,638,400 in IgG ELISA).

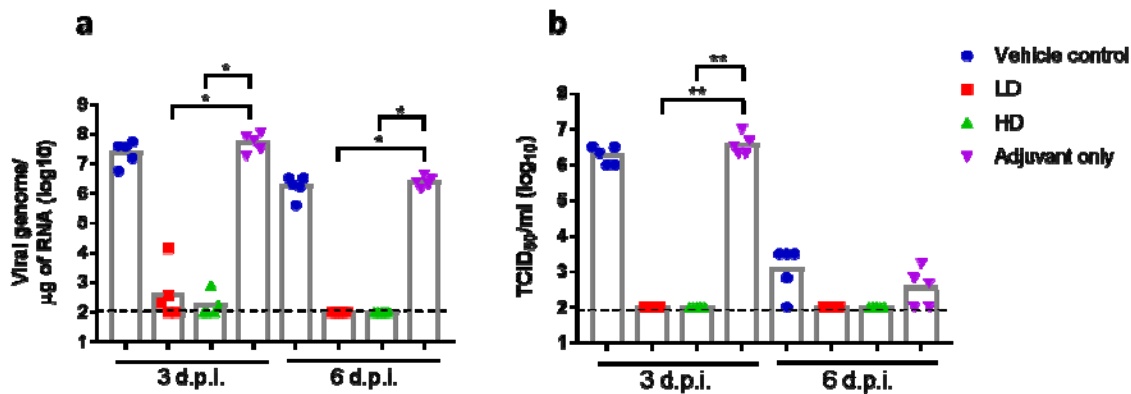


354

355 **Figure 3. Change in body weight in hamsters after infection with SARS-CoV-2.**

356 Hamsters immunized in Figure 2 were challenged with 10^4 PFU virus. The body weights of individual
357 hamsters were tracked daily up to the time of euthanizing at 3 d.p.i. (n = 5 per group) and 6 d.p.i. (n = 5 per
358 group). Results are presented as mean with error bars representing standard error and statistical significance
359 calculated with Two-way ANOVA with Tukey's multiple comparison test at 3 d.p.i. (left) or 6 d.p.i. (right).

360

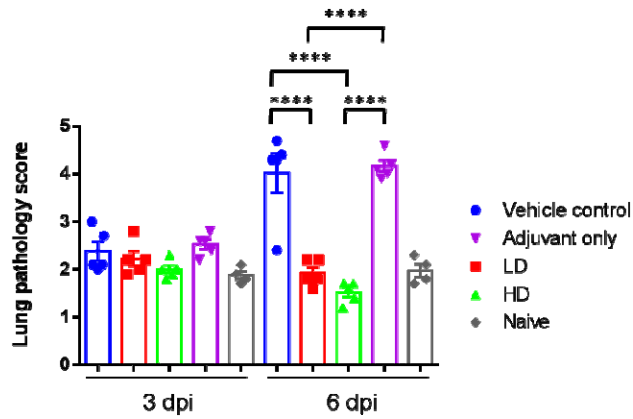


361

362 **Figure 4. Viral load in hamsters 3 or 6 days post infection with SARS-CoV-2.**

363 The hamsters were euthanized at 3 or 6 d.p.i. and lung tissue samples were collected for viral load
364 determination by **a.** quantitative PCR of viral genome RNA, and **b.** TCID₅₀ assay for virus titer. Results are
365 presented as geometric mean with error bars representing 95% confidence interval and statistical significance
366 calculated with Kruskal-Wallis with corrected Dunn's multiple comparisons test. Dotted lines represent lower
367 and limit of detection (100).

368



369

370 **Figure 5. Lung pathology scoring in hamsters 3 or 6 days post infection with SARS-CoV-2.**

371 The hamsters were euthanized at 3 or 6 d.p.i. and lung tissue samples were collected for sectioning and
372 staining. The histopathology sections were scored as outlined in the methods and the results tabulated. Results
373 are presented as mean of lung pathology scores with error bars representing standard error and statistical
374 significance calculated with one-way ANOVA with Tukey's multiple comparisons test.